

Cell penetration properties of maurocalcine, a natural venom peptide active on the intracellular ryanodine receptor

Sylvie Boisseau¹, Kamel Mabrouk², [Ram Narendra](#)¹, Nicolas Garmy³,
Véronique Collin⁴, Abir Tadmouri¹, Mohamad Mikati⁵, Jean-Marc Sabatier²,
Michel Ronjat¹, Jacques Fantini³ and Michel De Waard^{1#}

¹Inserm U607, Canaux Calciques, Fonctions et Pathologies, 17 rue des Martyrs, 38054 Grenoble Cedex 09, France ; CEA, Grenoble, France ; Université Joseph Fourier, Grenoble, France.

²CNRS FRE 2738, Laboratoire Ingénierie des Protéines, Boulevard Pierre Dramard, 13916 Marseille Cedex 20, France.

³UMR-INRA 1111, Laboratoire de Biochimie et Physicochimie des Membranes Biologiques, Avenue Escadrille Normandie-Niemen, 13397 Marseille Cedex 20, France.

⁴INSERM U548, Laboratoire d'Immunochimie, 17 rue des Martyrs, 38054 Grenoble Cedex 9, France.

⁵Department of Pediatrics, American University of Beirut Medical Center, Beirut, Lebanon.

Send correspondence to Dr. Michel De Waard:

Tel.: (33) 4 38 78 68 13

Fax: (33) 4 38 78 50 41

E-mail: mdewaard@cea.fr

Abstract

Maurocalcine (MCA) is a 33 amino acid residue peptide toxin initially isolated from the scorpion *Scorpio maurus palmatus*. Its structural and functional features make it resembling many Cell Penetrating Peptides. In particular, MCA exhibits a characteristic positively charged face that may interact with membrane lipids. External application of MCA is known to produce Ca^{2+} -release from intracellular stores within seconds. MCA binds directly to the skeletal muscle isoform of the ryanodine receptor, an intracellular channel target of the endoplasmic reticulum, and induces long-lasting channel openings in a mode of smaller conductance. The binding sites for MCA have been mapped within the cytoplasmic domain of the ryanodine receptor. In this manuscript, we further investigated how MCA proceeds to cross biological membranes in order to reach its target. A biotinylated derivative of MCA (MCA_b) was chemically synthesized, coupled to a fluorescent streptavidine indicator (Cy3 or Cy5) and the cell penetration of the entire complex followed by confocal microscopy and FACS analysis. The data provide evidence that MCA allows the penetration of the macro proteic complex and therefore may be used as a vector for the delivery of proteins in the cytoplasm as well as in the nucleus. Using both FACS and confocal analysis, we show that the cell penetration of the fluorescent complex is observed at concentrations as low as 10 nM, is sensitive to membrane potential and is partly inhibited by heparin. We also show that MCA interacts with the disialoganglioside GD3, the most abundant charged lipid in natural membranes. Despite its action on ryanodine receptor, MCA showed no sign of cell toxicity on HEK293 cells suggesting that it may have a wider application range. These data indicate that MCA may cross the plasma membrane directly by cell translocation and has a promising future as a carrier of various drugs and agents of therapeutic, diagnostic and technological value.

Keywords: Cell-penetrating peptides; Cellular uptake; Maurocalcine; Cargo delivery.

Abbreviations: MCA, maurocalcine; MCA_b, biotinylated maurocalcine; Strep, streptavidine; Cy3, cyanine 3; Cy5, cyanine5; GD3, disialoganglioside NeuAc α 2-8NeuAc α 2-3Gal β 1-4Glc β 1-Cer; DPPC, dipalmitoylphosphatidylcholine; DHPR, dihydropyridine receptor; RyR, ryanodine receptor; SR, sarcoplasmic reticulum; PBS, phosphate buffered-saline; CPP, cell penetrating peptide.

1. Introduction

Maurocalcine (MCA) is a 33 amino acid residue peptide that was initially isolated from the venom of the chactid scorpion *Scorpio maurus palmatus* [1] (Fig. 1A). Since then, it has been chemically synthesized without any loss in pharmacological activity or structural alteration [2]. The peptide is cross-linked by three disulfide bridges according to the pattern: Cys³-Cys¹⁷, Cys¹⁰-Cys²¹ and Cys¹⁶-Cys³² [2]. The 3-D structure of MCA, determined in solution by ¹H-NMR [3], shows an inhibitor cystine knot motif [4] and three β -strands running from amino acid residues 9-11 (strand 1), 20-23 (strand 2) and 30-33 (strand 3), respectively. The β -strands 2 and 3 form an antiparallel sheet. MCA is a highly basic peptide since 12 out of 33 residues are positively charged, including the amino terminal Gly residue, seven Lys residues and four Arg residues (Fig. 1B). In contrast, MCA contains only four negatively charged residues, meaning that the global net charge is positive. A representation of the electrostatic surface potential of MCA demonstrates that MCA presents a basic face in which the first Gly residue and all Lys residues are involved (Fig. 1C, left panel). Interestingly, none of the four Arg residues are involved in this basic face. The rest of the molecule is mainly hydrophobic (Fig. 1C, right panel), meaning that MCA is a strongly polarized molecule and possesses an important dipole moment. Three relative peptides have been isolated or cloned from the venoms of different scorpions: imperatoxin A [5], from the scorpion *Pandinus imperator*, that shares 82% sequence identity with MCA, and both opicalcine 1 and 2 [6], from the scorpion *Opisthophthalmus carinatus*, that show higher 91% and 88% sequence identities, respectively (Fig. 1B). In these three analogues, amino acid substitutions did not alter the net global charge of the peptides.

MCA and imperatoxin A have initially triggered interest for two reasons. First, they are potent activators of the ryanodine receptor (RyR), a calcium channel responsible for the release of calcium from intracellular stores [5,7]. Indeed, both toxins bind with nanomolar affinity onto the skeletal muscle isoform of the RyR inducing an increase in opening probability and the appearance of long-lasting openings of the channel at a sub-maximal conductance state. These effects are responsible for the property of MCA to induce calcium release from the sarcoplasmic reticulum (SR) [2,8,9]. Moderate effects of imperatoxin A have been reported on the cardiac (type 2) and brain (type 3) RyR isoforms as well [10,11]. Interestingly, application of MCA in the extracellular medium of cultured myocytes triggers, within seconds, a transient calcium release from the SR intracellular store [7]. Second, both toxins present some sequence homology with a cytoplasmic sequence (termed domain A) of

the pore-forming subunit of the dihydropyridine (DHP)-sensitive voltage-gated calcium channel of skeletal muscle (DHP receptor, DHPR) [7,12]. This homology is located in a DHPR region known to be important for the mechanical coupling between the DHPR and RyR, a physiologically process required for SR calcium release and therefore muscle contraction. Besides this sequence homology, it has been proposed that the β -sheet structure of the MCa and imperatoxin could mimic the helical structure of domain A [13]. In addition, a peptide of domain A, MCa and imperatoxin A were all shown to induce similar modifications in RyR channel properties [2,8,9]. Peptide A was found to block at least some effects of MCa [8] or imperatoxin A [14]. Finally, we recently demonstrated that MCa and peptide A share common binding sites on RyR [15]. As such, MCa and its related analogues are interesting peptide tools for dissecting the molecular events that lead to muscle contraction [16]. [Fig. 2](#) summarizes the major aspects of these findings.

Given the location of the site of pharmacological action of MCa and its analogues, combined with the rapid effect of MCa on cultured myocytes Ca^{2+} homeostasis upon external application, these peptides ought to efficiently cross the plasma membrane through a process faster than endocytosis. Therefore, these peptides now become interesting for a third reason: they may be derived for technological purposes in order to favor the membrane translocation of non-permeable molecules or nano-compounds. Proof that MCa translocates across the plasma membrane was recently provided by using a biotinylated derivative of MCa (MCa_b) that was coupled to a fluorescent derivative of streptavidine (Strep) [17]. Indeed, we showed that the MCa_b -Strep complex efficiently penetrates into various cell types without requiring metabolic energy or endocytosis. This penetration was rapid and reached saturation within 20 min for an external MCa concentration of 100 nM. MCa appears to share several traits with other cell penetrating peptides (CPPs) such as the HIV-encoded transactivator of transcription (Tat) [18], the insect transcription factor Antennapedia (Antp, also termed penetratin) [19], the herpes virus protein VP22 that regulates transcription, the chimeric peptide transportan [20] made in part by the neuropeptide galanin and by the wasp venom peptide mastoparan, and polyarginine peptides [21]. MCa has in common with these peptides the following characteristics: 1) it is a small peptide, 2) it is heavily charged, 3) it penetrates efficiently in all cell types and in 100% of the treated cells, 4) its penetration is fast and doesn't require cell energy suggesting that it can penetrate without an endocytosis-type mechanism, 5) its penetration doesn't apparently require the presence of cell surface receptors, and 6) MCa can carry high molecular weight cargoes during the penetration process. The CPPs have proven invaluable for the efficient cell penetration of oligonucleotides [22], plasmids [23], antisense

peptide nucleic acids [24], peptides [25], proteins [26,27], liposomes [28] and nanoparticles [29]. CPPs open the door to important new applications: antisense strategies for pain treatment [24], novel probes for intracellular magnetic labeling both *in vitro* and *in vivo* [30], brain delivery of antineoplastic agents [31] or other therapeutic biomolecules [32], delivery of cyclosporine A for inhibition of cutaneous inflammation [33], etc. Because M_{Ca} appears to represent the first known natural disulfide-bridged cell penetrating peptide that possesses a well identified intracellular target, we further characterized its properties of cell penetration. We investigated the concentration dependence of M_{Ca} penetration, its cell toxicity and its mechanism of penetration. For the latter, we studied i) the effect of transmembrane potential variation onto the penetration and ii) the affinity of M_{Ca} for various membrane lipids. The data obtained further strengthen the hypothesis that M_{Ca} reaches its pharmacological target by entering cells through a translocation mechanism. The lack of cell toxicity of this peptide vector, combined with the availability of pharmacologically inactive analogues, suggest that M_{Ca} derivatives will permit future promising technological and medical applications.

2. Materials and methods

2.1. Materials

The disialoganglioside NeuAc α 2-8NeuAc α 2-3Gal β 1-4Glc β 1-Cer (GD3) and dipalmitoylphosphatidylcholine (DPPC) were purchased from Matreya Inc and Sigma, respectively.

2.2. M_{Ca} and M_{Ca_b} peptide synthesis

The chemical syntheses of M_{Ca} and its biotinylated derivative M_{Ca_b} were performed as previously described [2,17].

2.3. Cell culture

HEK293 (human embryonic kidney cells, ATCC) were maintained at 37°C in 5% CO₂ in DMEM (Dulbecco's modified Eagle's medium, InVitrogen) supplemented with 10% (v/v) heat-inactivated foetal bovine serum (InVitrogen) and 10.000 units/ml streptomycine and penicillin (InVitrogen).

2.4. Formation of the M_{Ca_b}-Streptavidin-Cyanine3/5 complex

Soluble streptavidin-cyanine 5 or streptavidin-cyanine 3 (Strep-Cy5 or Strep-Cy3, Amersham Biosciences) was mixed with four molar equivalents of M_{Ca_b} for 2 hours at 37°C in the dark, in phosphate-buffered saline (PBS, in mM: NaCl 136, Na₂HPO₄ 4.3, KH₂PO₄ 1.47, KCl 2.6, CaCl₂ 1, MgCl₂ 0.5, pH 7.2).

2.5. Flow cytometry

After 1 hr incubation with M_{Ca_b}-Strep-Cy5 complexes, the cells were washed twice with PBS to remove extracellular complexes, and, where indicated, treated with 1 mg/ml trypsin (InVitrogen) for 10 min at 37°C to remove cell surface-bound complexes. After trypsin incubation, the cell suspension was centrifuged at 500 g and cells were resuspended in PBS containing 1 µg/ml of propidium iodide (Sigma). For experiments that did not include a step with propidium iodide (dose-response data), the M_{Ca_b}-Strep-Cy3 complex was used instead of M_{Ca_b}-Strep-Cy5.

For experiments with heparin-treatment, complexes were prepared in PBS containing 10 µg/ml of heparin (heparin sodium from bovine intestinal, Sigma). The complexes were then incubated with cells. Cells were rinsed twice with the PBS solution that contains heparin before and after incubation with the M_{Ca} complexes.

For experiments in which the KCl concentration gradient was altered to induce cell depolarization, the M_{Ca} complexes were prepared in solutions with variable NaCl / KCl ratios (composition in mM: NaCl 145 to 5, KCl 5 to 145, CaCl₂ 2.5, MgCl₂ 1.2, Glucose 10, HEPES 10, pH 7.4). Before and after incubation with M_{Ca} complexes, cells were rinsed twice with these different solutions.

Flow cytometry analyses, under all these different experimental conditions, were performed with live cells using a Becton Dickinson FACSCalibur flow cytometer (BD Biosciences). Data were obtained and analysed using CellQuest software (BD Biosciences). Live cells were gated by forward/side scattering from a total of 10.000 events.

2.6. MTT assay

HEK293 cells were seeded into 96 well micro plates at a density of approximately 5,000 cells/well. Then the cells were incubated in suspension with different concentrations of M_{Ca} up to a maximum of 10 µM at 37°C for a period of 4 or 24 hrs. In addition to M_{Ca}, control wells with or without cells in cell culture medium were included for each experiment. All assays were run in triplicates.

The cell viability was measured using the Cell Quanti-MTT assay Kit (Bioassay, USA). Here, the conversion of 3-(4,5-dimethylthiazol-2-yl)-2,5-diphenyl-tetrazolium bromide (MTT) into purple colored MTT formazan by the living cells indicates the extent of cell viability. The optical density was measured at 570 nm using the FLUOstar OPTIMA microplate reader (BMG Labtech) followed by analyses.

2.7. Immunocytochemistry

For analysis of the subcellular localization of the M_{Ca}_b-Strep-Cy3 complexes, following complexes application, cells were fixed 10 min in 4% paraformaldehyde, rinsed in PBS and incubated for 1 hr with FITC-conjugated Concanavalin A (Molecular Probes, 5 µg/ml) to stain the membrane and with TO-PRO-3 iodide (Molecular Probes, 1 µM) to stain the nucleus. For staining of cytoskeleton, cells were fixed and permeabilized with cold methanol for 10 min, rinsed twice in PBS and incubated for 2 hrs with a mouse anti- α -tubulin antibody (1:1000, Sigma). After two washes in PBS, cells were incubated for 1 hour with Alexa 488-conjugated-anti-mouse IgG antibody (1:1000, Molecular Probes). Cells were then mounted in Vectashield mounting medium (Vector laboratories). Preparations were analyzed by confocal laser scanning microscopy using a Leica TCS-SP2 operating system. Alexa-488 and Cy3 or propidium iodide fluorescences were sequentially excited and collected. Images were merged in Adobe Photoshop 7.0

2.8. Surface pressure measurements

The surface pressure was measured with a fully automated microtensiometer (μ TROUGH SX, Kibron Inc.). The apparatus allowed the recording of the kinetics of interaction of a ligand with a monomolecular film using a set of specially designed Teflon troughs. All experiments were carried out in a controlled atmosphere at $20 \pm 1^\circ\text{C}$. Monomolecular films of the indicated lipids were spread on ultra-pure water subphases (volume of 800 µl) from hexane:chloroform:ethanol (11:5:4, v/v/v) as described previously [34]. After spreading of the film, a minimal lapse time of 5 min was awaited to allow solvent evaporation. To measure the interaction of M_{Ca} with lipid monolayers, various concentrations of the peptide were injected in the subphase with a 10 µl Hamilton syringe, and the resulting pressure increases produced by peptide incorporation were recorded until reaching the equilibrium (maximal surface pressure increase usually obtained after 100–150 min of interaction). For the dose-dependent interaction between M_{Ca} and GD3, the monomolecular films of GD3 were prepared at an initial surface pressure (p_i) of $10 \text{ mN}\cdot\text{m}^{-1}$. The data were analyzed with the Filmware 2.5

program (Kibron Inc.). The accuracy of the system for surface pressure measurements was $0.25 \text{ mN}\cdot\text{m}^{-1}$ under our experimental conditions.

3. Results

3.1. Cell distribution of $\text{MCA}_b\text{-Strep-Cy5}$ and time-dependent re-distribution towards the nucleus

In a former study, we have demonstrated that $\text{MCA}_b\text{-Strep-Cy3}$ complexes enter efficiently in the cytoplasm of various living cell types [17]. Cell entry was not prevented by inhibitors of endocytosis or pinocytosis or by incubation at 4°C . Cell fixation also did not appear to alter the cellular distribution of the complex even though it appears more questionable for other CPPs [35]. Here, we further investigated by confocal microscopy the cell distribution of $\text{MCA}_b\text{-Strep-Cy5}$ in HEK293 cells after 1 hr incubation of the cells with 333 nM of the complex (Fig. 3). Surface labeling of HEK293 cells was performed with concanavalin A whereas the nuclei of cells were labeled with propidium iodide (Fig. 3A). Comparison of these labeling with that of $\text{MCA}_b\text{-Strep-Cy5}$ clearly illustrate the presence of the latter at both the plasma membrane and inside the cytoplasm of cells. The staining of the complex appeared somewhat punctuate in a confocal plane. Preliminary data seem to suggest that this punctuate distribution appears related to the presence of streptavidine. This protein may possibly non specifically associate to endogenous cell proteins. This question will need to be addressed separately. We also performed a comparison of the distribution of $\text{MCA}_b\text{-Strep-Cy5}$ with that of α -tubulin, a marker of the cytoskeleton. A clear lack of colocalization is evidenced (Fig. 3B) between this cytoskeleton marker and $\text{MCA}_b\text{-Strep-Cy5}$ complex. The diffuse staining of α -tubulin was linked to the use of HEK293 cells since a similar staining was observed in the absence of MCA and also with different commercial antibodies (data not shown). We next followed the evolution as a function of time of the cellular distribution of the $\text{MCA}_b\text{-Strep-Cy3}$ complex (Fig. 3C). After 2 hrs of incubation, the complex was mostly present in the cytoplasm. Between 4 and 24 hrs of incubation, it was mostly perinuclear and colocalized with the nucleus. The regular target of MCA is RyR, and the site of binding of MCA on RyR is strictly localized in the cytoplasm. The localization of the $\text{MCA}_b\text{-Strep-Cy3}$ in the nucleus cannot result from its binding onto RyR. Using a specific pull-down assay with Strep-polystyrene beads and MCA_b as a bait for interaction with cDNA, we evidenced that MCA_b does not interact with cDNA (data not shown). Thus, the presence of $\text{MCA}_b\text{-Strep-Cy3}$ complex in the nucleus does not seem to arise from an interaction with DNA.

3.2. Study of the cell penetration and cell toxicity of M_{Ca_b}-Strep-Cy5 by FACS

FACS is an interesting method to work out the quantitative aspects of M_{Ca_b}-Strep-Cy5 penetration on live cells. However, FACS analysis does not allow distinguishing between cell surface bound fluorescence and intracellular fluorescence. Cell surface fluorescence is expected to arise from M_{Ca_b}-Strep-Cy5 complexes bound onto the outer face of the plasma membrane, through electrostatic interactions with either lipids, or specific protein receptors or proteoglycans. In order to destroy the M_{Ca_b}-Strep-Cy5 complex present on the external face of the membrane and to measure only the fluorescent signal corresponding to the penetrated complex, cells were treated with trypsin before FACS analysis. Interactions of different CCPs, such as Tat, with proteoglycans have been described previously [36]. We then investigated the effect of pre-incubating M_{Ca_b}-Strep-Cy5 with heparin on the cell penetration of the fluorescent complex. Heparin is one of the major glycosaminoglycans that form the polysaccharide chain of the proteoglycans and therefore should competitively displace the interactions of the M_{Ca_b}-Strep-Cy5 with proteoglycans. However, binding of heparin on M_{Ca_b} may also non-specifically hinder the translocation of the M_{Ca_b}-Strep-Cy5 complex by neutralizing the positive charges provided by the basic residues of M_{Ca_b}. Fig. 4A (left panel) shows that the incubation of M_{Ca_b}-Strep-Cy5 with 10 µg/ml heparin before and during cell incubation significantly decreased the cell fluorescence. The mean fluorescence value was decreased from a value of 307 (arbitrary units) in the absence of heparin to a value of 78. Further treatment of the cells with 1 mg/ml trypsin to remove the surface bound M_{Ca_b}-Strep-Cy5 associated fluorescence had only a minor effect by further decreasing the mean fluorescence value to 64 (Fig. 4A, right panel). These data indicate that heparin can significantly decrease M_{Ca_b} uptake by cells either by hindering its interaction with proteoglycans or by altering its properties of interaction with negatively charged lipids by binding to its basic face. However a significant part of the M_{Ca_b}-Strep-Cy5 is still internalized in the presence of heparin. The data also show that surface associated M_{Ca_b}-Strep-Cy5 complexes are of limited quantities compared to intracellular complexes. Nevertheless, since it is clear that FACS analysis can be validly used for studying cellular uptake of CPPs only when a protease digestion step is included, (see also [35]), we thus performed all the subsequent analyses by including a trypsin digestion before FACS measurements.

We next determined whether 1 hr incubation with M_{Ca_b} alone or M_{Ca_b}-Strep-Cy5 could be toxic for HEK293 cells by measuring the incorporation of propidium iodide on the

total cell population (Fig. 4B). The incorporation of propidium iodide that witnesses cell death was compared to the one obtained in the absence of M_{Ca_b}. Statistically, no differences were found between Strep-Cy5 and M_{Ca_b}-Strep-Cy5 for concentrations up to 1 μM. The example shown in Fig. 4B is the most unfavorable case that we observed with most other cases ranging between 3 and 7% propidium iodide positive cells. For M_{Ca_b}-Strep-Cy5 concentrations higher than 1 μM, cell toxicity was observed but it was related to the presence of Strep-Cy5, since this effect was not observed when high concentrations of M_{Ca_b} alone (higher than 1 μM) were used (data not shown). The absence of M_{Ca} toxicity on HEK293 cells validates the use of this cell model for the study of internalization of M_{Ca}. However, this lack of toxicity may be related to the low expression of RyR1 in this cell line and needs to be controlled in different cell type.

Since for periods of incubation longer than 1 hr, M_{Ca} could be detected also in the nucleus, there is a possibility that cell toxicity may be a late phenomenon. We therefore also examined whether cells were sensitive to a prolonged exposure to M_{Ca} (4 hrs and 24 hrs incubation periods). M_{Ca} was tested alone since potential toxic effects of streptavidine were without cellular interest. HEK293 cell viability was measured using the Cell Quanti-MTT assay Kit from Bioassay corporation. As shown in Fig. 4C, there was absolutely no sign of significant cell toxicity for M_{Ca} concentrations up to 5 μM whether the incubation time lasted 4 hrs or 24 hrs. Only 8.0 ± 1.4 % cell toxicity was detected for an M_{Ca} concentration of 10 μM and a 24 hrs incubation time.

3.3. Dose-dependent penetration of M_{Ca_b}-Strep-Cy3 in HEK293 cells

Since M_{Ca_b} appears to act as an efficient CPP, we next determined the dose-dependence of cell penetration of the M_{Ca_b}-Strep-Cy3 complex. A mechanism of penetration that would rely on endocytosis would be expected to saturate, whereas a mechanism based on membrane translocation should be less prone to saturation. Fig. 5A illustrates that a detectable cell penetration is visible at a concentration as low as 10 nM, and that this penetration increases without any sign of saturation with increasing complex concentrations (Fig. 5B). The rather uniform increase in fluorescence values argues against the notion of two parallel mechanisms of penetration with widely different dose-dependencies. Confocal images confirm that cell penetration of the complex can occur of a wide range of concentration without any alteration in the cell distribution of the penetrated complex (Fig. 5C).

3.4. Voltage-dependence of M_{Ca_b}-Strep-Cy3 penetration in HEK293 cells

Penetration of the M_{Ca}_b-Strep-Cy3 complex through a membrane translocation process can be driven by two processes. First, the concentration gradient of the complex will drive the complex into the cell and act to equilibrate the external and internal concentrations. Second, M_{Ca} has a net global charge that is greatly positive and thus a negative membrane potential should favor M_{Ca} penetration. This second possibility was tested by altering the membrane potential of HEK293 cells by increasing external KCl concentrations. External NaCl concentrations were correspondingly reduced in order to preserve the solution osmolarity. Fig. 6A illustrates that increasing KCl concentrations produces a clear reduction in cell entry of the M_{Ca}_b-Strep-Cy3 complex. This reduction in cell entry was followed by plotting the mean cell fluorescence observed by FACS as a function of KCl concentration (Fig. 6B). The data indicate that there is a linear decrease in fluorescence intensity upon membrane depolarization demonstrating that membrane potential is involved in attracting M_{Ca} into the cells. However, at 145 mM KCl, a concentration where presumably all cells would be depolarized to 0 mV, we still observe a small penetration of the M_{Ca}_b-Strep-Cy3 complex that likely result of the concentration gradient.

3.5. M_{Ca} interaction with membrane lipids

To assess whether M_{Ca} could interact with specific membrane lipids, monomolecular films of DPPC and ganglioside GD3 were spread at the air-water interface. M_{Ca} was then added in the aqueous subphase at a concentration of 1 μM. The variations in the surface pressure of the film were then continuously recorded as a function of time (Fig. 7A). The data show that M_{Ca} is able to penetrate into the monolayer of GD3, as objectified by the large increase in surface pressure of the GD3 film. In contrast, M_{Ca} does not induce significant change in the surface pressure of the DPPC film, indicating that M_{Ca} does not recognize this glycerophospholipid. A dose-dependent interaction of M_{Ca} with lipid monolayers formed with ganglioside GD3 is shown in Fig. 7B. The interaction is clearly detectable at a concentration of 100 nM of M_{Ca} and reaches a maximum at 750 nM. The half-maximal effect was obtained at a concentration of 490 nM.

4. Discussion

4.1. The value of M_{Ca} for cell penetration of proteins

M_{Ca} appears as an interesting new candidate to serve as vector to mediate cell penetration of compounds that are otherwise unable to cross the plasma membrane. Because of the

localization of its natural pharmacological site, it leaves little doubt that it reaches the cytoplasm of cells. A pharmacological profiling of MCa has begun [7], and several point mutated analogues devoid of activity on RyR and Ca^{2+} homeostasis are already available. Along with the present observation that MCa is not toxic to HEK293 cells likely due to the poor expression of RyR in these cells, we expect that MCa analogues selected for their inability to bind RyR will be extremely useful as peptide vector for the cell penetration of compounds of interest. Consistent with a mechanism of cell penetration that does not require the presence of extracellular receptors, RyR-defective mutants of MCa proved to efficiently penetrate into cells (data not shown). Along with the observation that CPPs possess no clear sequence homology between each other, these data predict a great level of flexibility for the design of numerous MCa cell penetrating analogues. Nevertheless, the molecule in its actual configuration is not devoid of interesting features since: 1) a wide range of concentration can be exploited (as low as 10 nM for 1 hr incubation), 2) it induces entry of Strep, a protein as large as 60 kDa, 3) the cargo attains the cytoplasm as well as the nucleus which further widens the possible range of applications, and 4) it can enter many different cell types [17]. MCa not only favors the penetration of proteins, it also allows the penetration of 10-15 nm quantum dots coated with 5-7 Strep molecules each (unpublished data). This finding suggests that MCa will have many applications for *in vivo* cell tracking or other cell imaging techniques.

4.2. Interaction of MCa with lipids

Surface pressure measurements of MCa with monomolecular films of specific membrane lipids indicate that MCa can interact with gangliosides such as GD3, whereas it totally ignores DPPC. Therefore, these data suggest that the site of interaction of MCa with the external leaflet of plasma membranes may correspond to discrete areas enriched in negatively charged lipids such as gangliosides. Correspondingly, the lack of interaction of MCa with DPPC is consistent with the presence of a positive charge in the polar head group of this lipid, a property that should not be favourable for the numerous basic amino acids of MCa. In contrast, the positively charged peptide is expected to interact with negatively charged lipids. In the external leaflet of the plasma membrane, gangliosides are the most abundant lipids belonging to this category. Altogether, these data suggest that the initial interaction of MCa with plasma membranes occurs in gangliosides enriched domains. These domains may correspond to specific lipid rafts as previously suggested [37]. The only other candidate lipid that may possibly interact with MCa, phosphatidylserine, that is also negatively charged, is

mainly located at the cytoplasmic side of the membrane. An interaction of M_{Ca} with lipids does not provide a mechanism for the translocation of M_{Ca} across the plasma membrane. However, we may tentatively speculate that M_{Ca} / GD3 interactions neutralize the basic surface of M_{Ca} and favour the interaction of the hydrophobic face with the inner part of the membrane. Eventually, GD3 may translocate transiently from the outer part of the membrane towards the inner part in order to deliver M_{Ca} that may then prefer to establish new electrostatic interactions with novel, locally based, negatively charged lipids or proteins because of a richer environment in negative charges.

4.3. Endocytosis versus cell translocation

The question of the mechanism of cell penetration of CPPs appears to be hotly debated. Arguments have been put forward in favor of endocytosis, as well as for a pure energy independent membrane translocation mechanism. It is worth emphasizing that there is no contradiction for the coexistence of an endocytic pathway and a nonendocytic one. We discuss both issues.

Cell penetration of Tat has been demonstrated in experimental conditions in which cellular energy was depleted, temperature lowered, clathrin-dependent endocytosis inhibited, and cholesterol removed [38]. Arguments in favor of cell translocation of M_{Ca} are the observations that penetration also occurs at 4°C and upon treatment of cells with amiloride and nystatin [17]. The fact that the penetration of M_{Ca} does not saturate with increasing concentrations cannot be presented as an argument for a translocation mechanism since a non saturable step such as lipid interaction may be followed by endocytosis. Nevertheless, we provide two additional evidences in this manuscript for the non-endocytotic pathway. First, M_{Ca} cell entry is sensitive to membrane potential variation in manner coherent with the global net positive charge of M_{Ca}. To our knowledge, endocytosis is not known to be inhibited by voltage reduction. Second, M_{Ca} interacts with negatively charged membrane lipids, a condition that is required for any type of mechanism of translocation. Specificity of this interaction is demonstrated by the lack of association to a non-charged lipid. Interaction with negatively charged lipids was also observed for Antp [39]. The observation that cell fixation may influence the cell distribution of CPP renders the nonendocytic pathway difficult to defend [35]. However, this artifact of procedure may presumably be valid only for CPPs that are not conjugated to cargoes. In the present work, M_{Ca_b} was coupled to Strep, a quite large cargo of about 60 kDa, before cell entry. This is an important difference with several other studies in which the fluorescent complex is only formed after cell entry, fixation and

permeabilization. The present data also show that cell penetration can still be evidenced by FACS despite a treatment with trypsin. In fact, only a tiny fraction of MCA_b-Strep-Cy3 remains associated to the extracellular face of the membrane **when heparin is added** since trypsin treatment produces only a minimal reduction on cell penetration. In addition, the observation that there is a clear time-dependent evolution of the cell distribution of the MCA_b-Strep-Cy3 complex warrants against an artifact of cell fixation. **The presence of the complex in the nucleus after a period of 24 hrs is a strong indication that the peptide must be present in a free-form in the cytoplasm after a specific period.** Finally, we have not noticed any evident difference between experiments with live [17] and fixed cells. It should be emphasized that the most compelling argument in favor of cell translocation is the fact that MCA's pharmacological target has a strict cytoplasmic localization [15]. Also, the fast kinetics of MCA effects on calcium homeostasis is indicative that it reaches its binding site extremely rapidly, through a process that is largely incompatible with endocytosis [7]. In that respect, the coupling to a fluorescent Strep largely slows down the kinetic of cell entry. Electron microscopy studies with CPPs coupled to nanoparticles that are too large to undergo endocytosis will likely bring further evidence in favor of membrane translocation.

The observation that heparin treatment significantly inhibits MCA penetration into HEK293 cells may be in favor of an endocytic pathway. This may suggest that part of MCA cell penetration involves binding onto proteoglycans. We presume that it is the basic character of MCA that promotes its binding to negatively charged complex sulfated glycosaminoglycans of the cell surface. Although heparin may indeed competitively hinder MCA binding onto HPSG, and hence endocytosis, it may also non-competitively neutralize the basic face of MCA and partially block the interaction with negatively charged lipids and cell translocation. This issue will be resolved by examining cell penetration of MCA in proteoglycan-deficient cell lines. **Nevertheless, we cannot rule out that a significant fraction of MCA entry also occurs via lipid raft-dependent macropinocytosis, a specialized form of fluid phase endocytosis, that is independent of caveolae, clathrin and dynamin [40].**

4.4. Role of membrane potential

What drives the penetration of MCA into cells? There are two potential driving forces that can be evoked. Similarly to the cell penetration of ions through channels, MCA may rely on its concentration gradient that may be progressively neutralized during passive diffusion into the cell. In addition, since it possesses a net global charge of +8, it may also penetrate because of the negative potential of cells. This is indeed what we observed since the net amount of

M_{Ca}_b-Strep-Cy3 entry was lessened by membrane depolarization. As such, negative membrane potentials will act as “concentrators” of M_{Ca} into the cell, which may well explain why the associated cell fluorescence for M_{Ca}_b-Strep-Cy3 complexes was higher inside the cell than outside upon equilibrium [17]. Similarly, voltage-dependence of cell penetration has also been observed for the *Antennapedia*-derived penetratin [41]. In the case of penetratin, a significant increase in the rate of entry had been observed which is also expected. It will thus be interesting to check whether M_{Ca} entry is also accelerated by voltage.

4.5. Interesting parallels between M_{Ca} and peptide A and relevance to excitation-contraction coupling

The limited sequence homology between M_{Ca} and peptide A, combined with the observation that both peptides bind onto the same site of RyR [15] allow three interesting questionings. First, the observation that M_{Ca} cell entry is sensitive to the voltage gradient is particularly intriguing. The complex of channels that links the DHPR with RyR is highly sensitive to voltage changes. A modification in membrane potential is sensed by the DHPR and transduced to RyR to induce SR Ca²⁺ release. However, little is known about the identity of the DHPR sequence that is responsible for this voltage-sensitive transduction step. The domain A is an important determinant for the coupling between DHPR and RyR. It will therefore be of interest to investigate whether domain A presents some kind of voltage-dependence in its coupling to RyR. Second, the observation that M_{Ca} interacts with a negatively charged lipid, similarly raises the question on peptide A interaction with lipids and on the possible role of such an interaction on excitation-contraction coupling. Third, M_{Ca} appears to efficiently cross the plasma membrane. Peptide A is also positively charged and the question of a partial membrane penetration of this sequence that has a predicted cytoplasmic localization is thus also opened.

Acknowledgements

The authors wish to thank Mrs. Lissbeth Leon for technical help on experiments. We are indebted to Dr. Didier Grunwald for help in acquiring confocal images and to Dr. Serge Candeias for advise on the FACS analysis software.

References

- [1] A. Mosbah, R. Kharrat, J.G. Renisio, E. Blanc, J.M. Sabatier, M. El Ayeb, H. Darbon, 6ème Rencontre en Toxinologie, Paris (1998).
- [2] Z. Fajloun, R. Kharrat, L. Chen, C. Lecomte, E. Di Luccio, D. Bichet, M. El Ayeb, H. Rochat, P.D. Allen, I.N. Pessah, M. De Waard, J.M. Sabatier, Chemical synthesis and characterization of maurocalcine, a scorpion toxin that activates Ca^{2+} release channel/ryanodine receptors, FEBS Lett. 469 (2000) 179-185.
- [3] A. Mosbah, R. Kharrat, Z. Fajloun, J.G. Renisio, E. Blanc, J.M. Sabatier, M. El Ayeb, H. Darbon, A new fold in the scorpion toxin family, associated with an activity on a ryanodine-sensitive calcium channel, Proteins 40 (2000) 436-442.
- [4] P.K. Pallaghy, K.J. Nielsen, D.J. Craik, R.S. Norton, A common structural motif incorporating a cystine knot and a triple-stranded β -sheet in toxic and inhibitory polypeptides, Prot. Sci. 3 (1994) 1833-1839.
- [5] R. El Hayek, A.J. Lokuta, C. Arevalo, H.H. Valdivia, Peptide probe of ryanodine receptor function, Imperatoxin A, a peptide from the venom of the scorpion *Pandinus imperator*, selectively activates skeletal-type ryanodine receptor isoforms, J. Biol. Chem. 270 (1995) 28696-28704.
- [6] S. Zhu, H. Darbon, K. Dyason, F. Verdock, J. Tytgat, Evolutionary origin of inhibitor cystine knot peptides, FASEB J. 17 (2003) 1765-1784.
- [7] E. Estève, S. Smida-Rezgui, S. Sarkozi, C. Szegedi, I. Regaya, L. Chen, X. Altafaj, H. Rochat, P. Allen, I.N. Pessah, I. Marty, J.M. Sabatier, I. Jona, M. De Waard, M. Ronjat, Critical amino acid residues determine the binding affinity and the Ca^{2+} release efficacy of maurocalcine in skeletal muscle cell, J. Biol. Chem. 278 (2003) 37822-37831.
- [8] L. Chen, E. Estève, J.M. Sabatier, M. Ronjat, M. De Waard, P.D. Allen, I.N. Pessah, Maurocalcine and peptide A stabilize distinct subconductance states of ryanodine receptor type 1, revealing a proportional gating mechanism, J. Biol. Chem. 278 (2003) 16095-16106.
- [9] A. Tripathy, W. Resch, L. Xu, H.H. Valdivia, G. Meissner, Imperatoxin A induces subconductance states in Ca^{2+} release channels (ryanodine receptors) of cardiac and skeletal muscle, J. Gen. Physiol. 111 (1998) 679-690.
- [10] I. Simeoni, D. Rossi, X. Zhu, J. Garcia, H.H. Valdivia, V. Sorrentino, Imperatoxin A (IpTx_a) from *Pandinus imperator* stimulates [³H]ryanodine binding to RyR3 channels, FEBS Lett. 508 (2001) 5-10.
- [11] T. Nabhani, X. Zhu, I. Simeoni, V. Sorrentino, H.H. Valdivia, J. Garcia, Imperatoxin a enhances Ca^{2+} release in developing skeletal muscle containing ryanodine receptor type 3, Biophys. J. 82 (2002) 1319-1328.

- [12] C.W. Lee, E.H. Lee, K. Takeuchi, H. Takahashi, I. Shimada, K. Sato, S.Y. Shin, do H. Kim, J.I. Kim, Molecular basis of the high-affinity activation of type 1 ryanodine receptors by imperatoxin A, *Biochem. J.* 377 (2004) 385-394.
- [13] D. Green, S. Pace, S.M. Curtis, M. Sakowska, G.D. Lamb, A.F. Dulhunty, M.G. Casarotto, The three-dimensional structural surface of two beta-sheet scorpion toxins mimics that of an alpha-helical dihydropyridine receptor segment, *Biochem. J.* 370 (2003) 517-527.
- [14] A.F. Dulhunty, S.M. Curtis, S. Watson, L. Cengia, M.G. Casarotto, Multiple actions of imperatoxin A on ryanodine receptors: interactions with the II-III loop "A" fragment, *J. Biol. Chem.* 279 (2004) 11853-11862.
- [15] X. Altafaj, W. Cheng, E. Estève, J. Urbani, D. Grunwald, J.M. Sabatier, R. Coronado, M. De Waard, M. Ronjat, Maurocalcine and domain A of the II-III loop of the dihydropyridine receptor $Ca_v1.1$ subunit share common binding sites on the skeletal ryanodine receptor, *J. Biol. Chem.* 280 (2005) 4013-4016.
- [16] H. Szappanos, S. Smida-Rezgui, J. Cseri, C. Simut, J.M. Sabatier, M. De Waard, L. Kovacs, L. Csernoch, M. Ronjat, Differential effect of maurocalcine on Ca^{2+} release events and depolarization-induced Ca^{2+} release in rat skeletal muscle, *J. Physiol.* 565 (2005) 843-853.
- [17] E. Estève, K. Mabrouk, A. Dupuis, S. Smida-Rezgui, X. Altafaj, D. Grunwald, J.C. Platel, N. Andreotti, I. Marty, J.M. Sabatier, M. Ronjat, M. De Waard, Transduction of the scorpion toxin maurocalcine into cells – Evidence that the toxin crosses the plasma membrane, *J. Biol. Chem.* 280 (2005) 12833-12839.
- [18] A.D. Frankel, C.O. Pabo, Cellular uptake of the Tat protein from human immunodeficiency virus, *Cell* 55 (1988) 1189-1193.
- [19] D. Derossi, S. Calvet, A. Trembleau, A. Brunissen, G. Chassaing, A. Prochiantz, Cell internalization of the third helix of the Antennapedia homeodomain is receptor-independent, *J. Biol. Chem.* 271 (1996) 18188-18193.
- [20] M. Pooga, M. Hällbrink, M. Zorko, Ü. Langel, Cell penetration of transportan, *FASEB J.* 12 (1998) 67-77.
- [21] S.M. Fuchs, R.T. Raines, Pathway for polyarginine entry into mammalian cells, *Biochemistry* 43 (2004) 2438-2444.
- [22] A. Astriab-Fischer, D. Sergueev, M. fiscjer, B.R. Shaw, R.L. Juliano, Conjugates of antisense oligonucleotides with the Tat and antennapedia cell-penetrating peptides: effects on cellular uptake, binding to target sequences, and biologic actions, *Pharm. Res. (N.Y.)* 19 (2002) 744-754.
- [23] I.A. Ignatovich, E.B. Dizhe, A.V. Pavlotskaya, B.N. Akifiev, S.V. Burov, S.V. Orlov, A.P. Perevozchikov, Complexes of plasmid DNA with basic domain 47-57 of the HIV-1 tat protein are transferred to mammalian cells by endocytosis-mediated pathways, *J. Biol. Chem.* 278 (2003) 42625-42636.

- [24] M. Pooga, U. Soomets, M. Hällbrink, A. Valkna, K. Saar, K. Rezaei, U. Kahl, J.X. Hao, X.J. Xu, Z. Wiesenfeld-Hallin, T. Hökfelt, T. Bartfai, Ü. Langel, Cell penetrating PNA constructs regulate galanin receptor levels and modify pain transmission in vivo, *Nat. Biotech.* 16 (1998) 857-861.
- [25] N. Shibagaki, M.C. Udey, Dendritic cells transduced with protein antigens induce cytotoxic lymphocytes and elicit antitumor immunity, *J. Immunol.* 168 (2002) 2393-2401.
- [26] M. Rojas, J.P. Donahue, Z. Tan, Y.Z. Lin, Genetic engineering of proteins with cell membrane permeability, *Nat. Biotech.* 16 (1998) 370-375.
- [27] M. Pooga, C. Kut, M. Kihlmark, M. Hällbrink, S. Fernaeus, R. Raid, T. Land, E. Hallberg, T. Bartfai, Ü. Langel, Cellular translocation of proteins by transportan, *FASEB J.* 15 (2001) 1451-1453.
- [28] V.P. Torchilin, R. Rammohan, V. Weissig, T.S. Levchenko, TAT peptide on the surface of liposomes affords their efficient intracellular delivery even at low temperature and in the presence of metabolic inhibitors, *Proc. Natl. Acad. Sci. USA* 98 (2001) 8786-8791.
- [29] M. Lewin, N. Carlesso, C.H. Tung, X.W. Tang, D. Cory, D.T. Scadden, R. Weissleder, Tat peptide-derivatized magnetic nanoparticles allow in vivo tracking and recovery of progenitor cells, *Nat. Biotech.* 18 (2000) 410-414.
- [30] L. Josephson, C.H. Tung, A. Moore, R. Weissleder, High-efficiency intracellular magnetic labeling with novel superparamagnetic-Tat peptide conjugates, *Bioconjugate Chem.* 10 (1999) 186-191.
- [31] C. Rousselle, P. Clair, J.M. Lefauconnier, M. Kaczorek, J.M. Scherrmann, J. Tamsamani, New advances in the transport of doxorubicin through the blood-brain barrier by a peptide vector-mediated strategy, *Mol. Pharmacol.* 57 (2000) 679-686.
- [32] C. De Coupade, A. Fittipaldi, V. Chagnas, M. Michel, S. Carlier, E. Tasciotti, A. Darmon, D. Ravel, J. Kearsey, M. Giacca, F. Cailler, Novel human-derived cell-penetrating peptides for specific subcellular delivery of therapeutic biomolecules, *Biochem. J.* 390 (2005) 407-418.
- [33] J.B. Rothbard, S. Garlington, Q. Lin, T. Kirschberg, E. Kreider, P.L. McGrane, P.A. Wender, P.A. Khavari, Conjugation of arginine oligomers to cyclosporin A facilitates topical delivery and inhibition of inflammation, *Nat. Med.* 6 (2000) 1253-1257.
- [34] R. Mahfoud, N. Garmy, M. Maresca, N. Yahi, A. Puigserver, J. Fantini, Identification of a common sphingolipid-binding domain in Alzheimer, prion, and HIV-1 proteins, *J. Biol. Chem.* 277 (2002) 11292-11296.
- [35] J.P. Richard, K. Melikov, E. Vives, C. Ramos, B. Verbeure, M.J. Gait, L.V. Chernomordik, B. Lebleu, Cell-penetrating peptides. A reevaluation of the mechanism of cellular uptake, *J. Biol. Chem.* 278 (2003) 585-590.

- [36] M. Rusnati, G. Tulipano, E. Spillmann P. Tanghetti, P. Oreste, G. Zopetti, M. Giacca, M. Presta, Multiple interactions of HIV-1 Tat protein with size-defined heparin oligosaccharides, *J. Biol. Chem.* 274 (1999) 28198-28205.
- [37] K.A. Vyas, H.V. Patel, A.A. Vyas, R.L. Schnaar, Segregation of gangliosides GM1 and GD3 on cell membranes, isolated membrane rafts, and defined supported lipid monolayers, *Biol. Chem.* 382 (2001) 241-250.
- [38] P. Säälük, A. Elmquist, M. Hansen, K. Saar, K. Viht, Ü. Langel, M. Pooga, Protein cargo delivery properties of cell-penetrating peptides. A comparative study, *Bioconjugate Chem.* 15 (2004) 1246-1253.
- [39] M. Magzoub, L.E.G. Eriksson, A. Gräslund, Conformational states of the cell-penetrating peptide penetratin when interacting with phospholipid vesicles: effects of surface charge and peptide concentration, *Biochim. Biophys. Acta* 1563 (2002) 53-63.
- [40] I.M. Kaplan, J.S. Wadia, S.F. Dowdy, Cationic TAT peptide transduction domain enters cells by macropinocytosis, *J. Control. Rel.* 102 (2005) 247-253.
- [41] D. Terrone, S. Leung Wai Sang, J.R. Silvius, Penetratin and related cell-penetrating cationic peptides can translocate across lipid bilayers in the presence of a transbilayer potential, *Biochemistry* 42 (2003) 13787-13799.

Figure legends

Fig. 1. (A) *Scorpio maurus palmatus*, (B) amino acid sequence of MCa and (C) presentation of the basic face of MCa. (A) Image of the scorpion *Scorpio maurus palmatus* from which MCa has been isolated. (B) Sequence alignment of four analogous toxins, MCa, imperatoxin A, opicalcine 1 and opicalcine 2. The two first peptides are known to be active on the ryanodine receptor. Opicalcine and imperatoxin A are from different scorpion venoms. All four toxins have the same number of positively charged amino acid residues. (C) 3-D structure of MCa drawn by the WebLab ViewerPro software and surface coloured according to the electrostatic potential (blue and red represent positively and negatively charged amino acid residues, respectively). The basic face (right panel) depicts all positively charged residues of MCa (Gly¹, Lys⁸, Lys¹¹, Lys¹⁴, Lys¹⁹, Lys²⁰, Lys²² and Lys³⁰). The hydrophobic face illustrates the lack of positively charged amino acid residues on the opposite side of the molecule. The peptide backbone is depicted as a yellow ribbon, whereas only the lateral chains of positively charged amino acid residues are indicated with scaled balls and sticks.

Fig. 2. Schematic drawing of the ryanodine receptor (RyR). RyR is a calcium channel localized in the membrane of the endoplasmic reticulum. Its function is to produce calcium release from this internal calcium stock. MCa has a well identified binding site on RyR that is localized on the cytoplasmic side of the channel. Binding of MCa to its site on RyR triggers calcium release from endoplasmic reticulum vesicles and that can be measured by the change in fluorescence intensity of a calcium indicator as shown here (for details see [7]). [FKBP12: FK506 Binding Protein 12 kDa](#).

Fig. 3. Subcellular localization of MCa_b-Strep-Cy5 complexes studied by confocal immunofluorescence microscopy and compared to the localization of concanavalin A (A), α -tubulin (B), and as a function of time (C). (A) Subcellular localization of MCa_b-Strep-Cy5 complex (blue) in HEK293 cells compared to a marker of the plasma membrane. Cells were incubated 1 hr with 333 nM of MCa_b-Strep-Cy5. The plasma membrane is stained with concanavalin A (green) and the nuclei with propidium iodide (red). Images are from a single confocal plane. (B) As in (A) but for a comparison with a cytoskeleton marker (anti α -tubulin antibody, green). (C) Modifications in cell distribution of MCa_b-Strep-Cy3 complexes after cell translocation. Confocal Cy3 (red, MCa_b-Strep-Cy3 complexes) and To-PRO (blue, nuclei) fluorescence images of HEK293 cells incubated with 333 nM complexes for 2 hrs ([left](#)

panel), 4 hrs (middle panel) and 24 hrs (right panel). Note the progressive labelling of the nuclei by the M_{Ca_b}-Strep-Cy3 complexes.

Fig. 4. Effects of heparin and/or trypsin treatment on M_{Ca_b}-Strep-Cy5 cell penetration (A) and cell toxicity of the complexes (B, C) as assessed by FACS. (A) Incubation of HEK293 cells and of the M_{Ca_b}-Strep-Cy5 complex with 10 µg/ml heparin reduces cell penetration of the complex (left panel). Mean Cy5 fluorescence is 307 without treatment, whereas with heparin treatment, it drops down to 78. Treatment of cells and M_{Ca_b}-Strep-Cy5 with 10 µg/ml heparin combined with a cell treatment with 1 mg/ml trypsin further decreases the mean fluorescence value down to 64. Control fluorescence following treatment of cells with Strep-Cy5 alone reaches a mean value of 3.1 and is not influenced by trypsin or heparin treatment (not shown). M_{Ca_b}-Strep-Cy5 cell penetration was tested at a concentration of 1 µM. (B) Cell toxicity of 1 µM of Strep-Cy5 and of the M_{Ca_b}-Strep-Cy5 complex as assessed by iodide propidium cell incorporation. Iodide propidium positive cells are indicated in percentages. (C) Cell toxicity of M_{Ca} as assessed by the MTT test. HEK293 cells were incubated for 4 or 24 hrs in the presence of variable concentrations of M_{Ca}.

Fig. 5. Dose-dependent cell penetration of M_{Ca_b}-Strep-Cy3 complex (A-C). (A) FACS analysis of the cell penetration of the M_{Ca_b}-Strep-Cy3 complex at the indicated concentration. Cells underwent a trypsin treatment at 1 mg/ml before FACS analysis. (B) Mean cell fluorescence as a function of M_{Ca_b}-Strep-Cy3 concentration. Data were fitted with the following equation $y = y_0 + a \times (1 - \exp(-b \times x))$ where $y_0 = -3.8$, $a = 199$ and $b = 1.5 \times 10^{-3}$. (C) Confocal immunofluorescence images of HEK293 cells incubated for 1 hr with different concentrations of M_{Ca_b}-Strep-Cy3 complexes (red). Nuclei are stained with To-PRO-3 (blue).

Fig. 6. Effect of increasing extracellular K⁺ concentrations on M_{Ca_b}-Strep-Cy3 cell penetration (A, B). (A) FACS analyses of the effects of increasing KCl concentrations on M_{Ca_b}-Strep-Cy3 cell penetration. Right panels illustrate control experiments (cell fluorescence without any complex, top, and cell fluorescence with Strep-Cy3) at 145 mM KCl. The KCl gradient had no effect on control values (not shown). Left panels illustrate the effects of 5 mM (top, mean cell fluorescence value of 145), 125 mM (middle, mean cell fluorescence value of 40) and 145 mM KCl (bottom, mean cell fluorescence value of 17), respectively. (B) Evolution of the mean cell fluorescence as a function of KCl concentration.

Linear regression of the data with $y = y_0 + a \times x$ with the maximum fluorescence $y_0 = 139.5$ and the descending slope $a = -0.72$.

Fig. 7. Interaction of MCa with membrane lipids (A, B). (A) Surface pressure measurement with monomolecular films of GD3 or DPPC. Kinetics of changes in surface pressure induced by the application of 1 μM MCa. The data illustrate the interaction of MCa with GD3 but not DPPC. The initial surface pressure was approximately 10 $\text{mN}\cdot\text{m}^{-1}$. The data were fitted with an exponential rise to max equation $y = y_0 + a \times (1 - \exp(-b \times x))$ where the initial surface pressure of the film is $y_0 = 11.6 \text{ mN}\cdot\text{m}^{-1}$, the maximal increase in surface pressure $a = 22.9 \text{ mN}\cdot\text{m}^{-1}$ and the time constant of surface pressure change $b = 3 \times 10^{-4} \text{ sec}^{-1}$. (B) Evolution of surface pressure of GD3 lipid films as a function of MCa concentration. Data were fitted with a sigmoid function $y = a / (1 + \exp(-(x-x_0)/b))$ where the maximum surface pressure increase $a = 22.1 \text{ mN}\cdot\text{m}^{-1}$, the slope $b = 0.006$ and the half-maximal effect occurs at a concentration of $x_0 = 0.49 \mu\text{M}$.

A

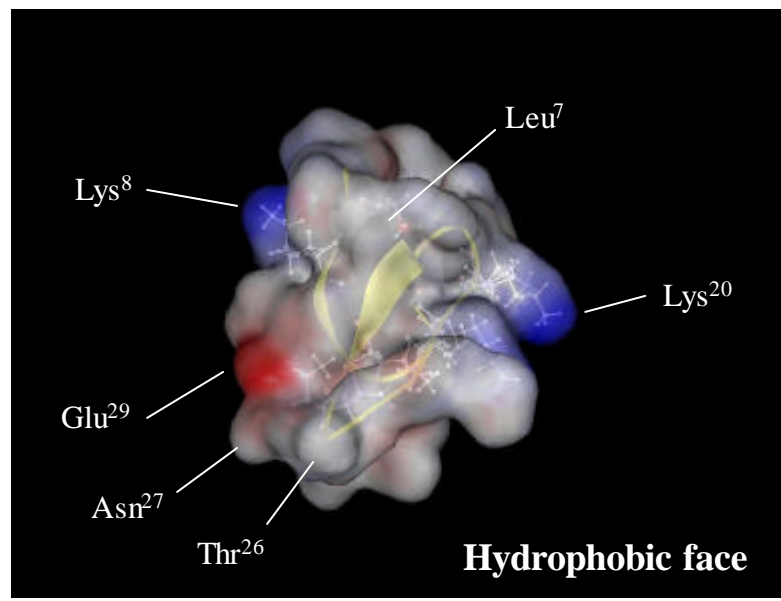
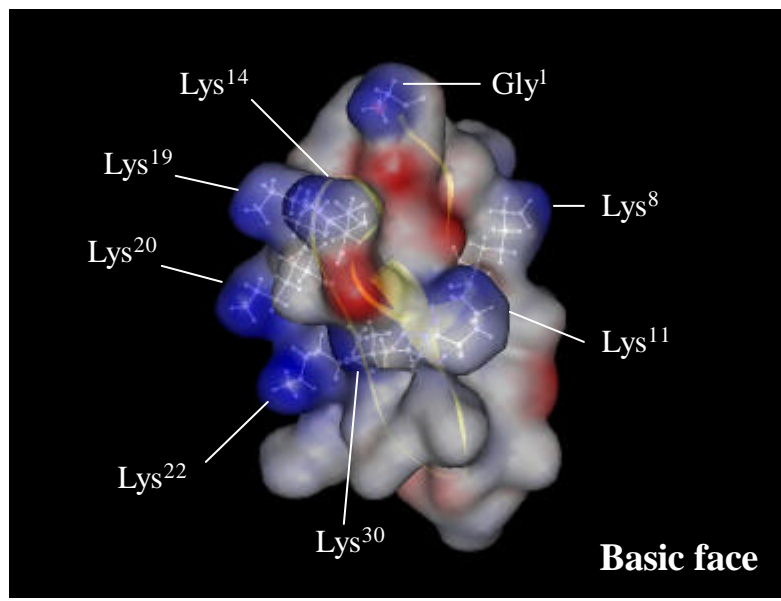


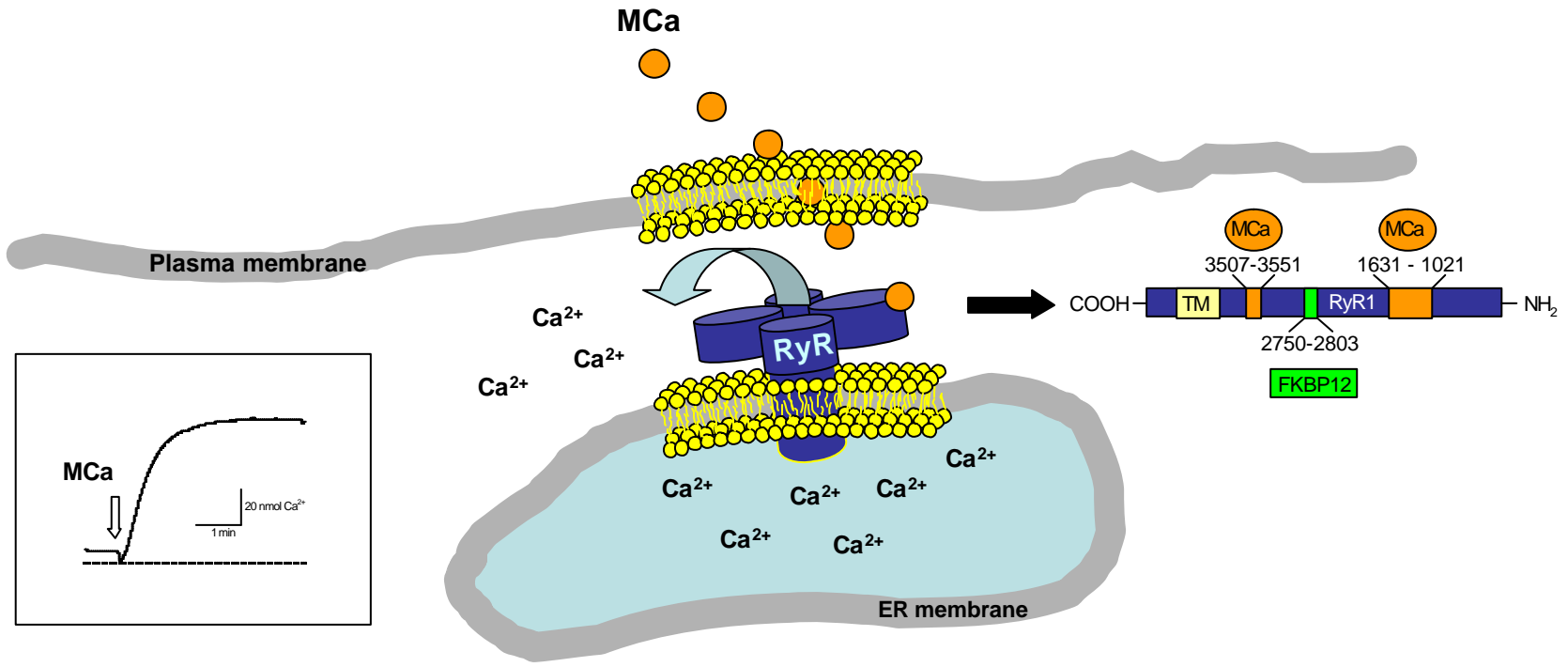
B

	Variable amino acid residues							
	1	2	3	4	5	6	7	
Maurocalcine	GDC ₁	LPHLKLC ₂	KENKDC ₃	C ₄	SKKC ₅	KRRGTNIEKRC ₆	R	12/33
Imperatoxin A	GDC ₁	LPHLKRC ₂	KADNDC ₃	C ₄	GKKC ₅	KRRGTNAEKRC ₆	R	12/33
Opicalcine 1	GDC ₁	LPHLKRC ₂	KENNDCC ₃	C ₄	SKKC ₅	KRRGTNPEKRC ₆	R	12/33
Opicalcine 2	GDC ₁	LPHLKRC ₂	KENNDCC ₃	C ₄	SKKC ₅	KRRGANPEKRC ₆	R	12/33

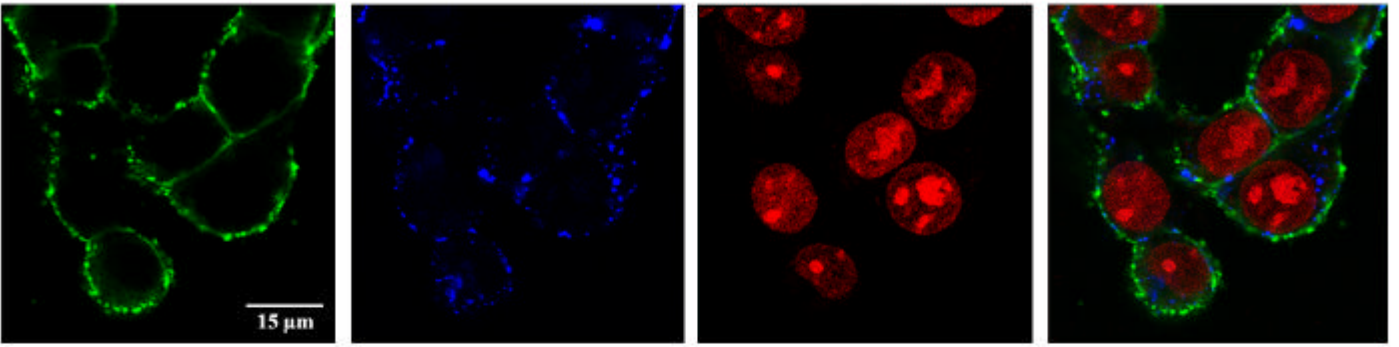
Number of basic residues

C

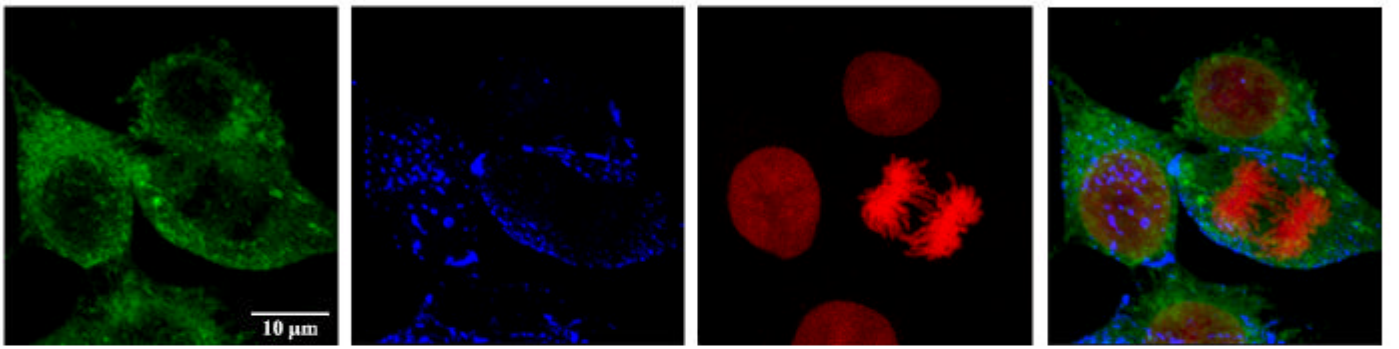




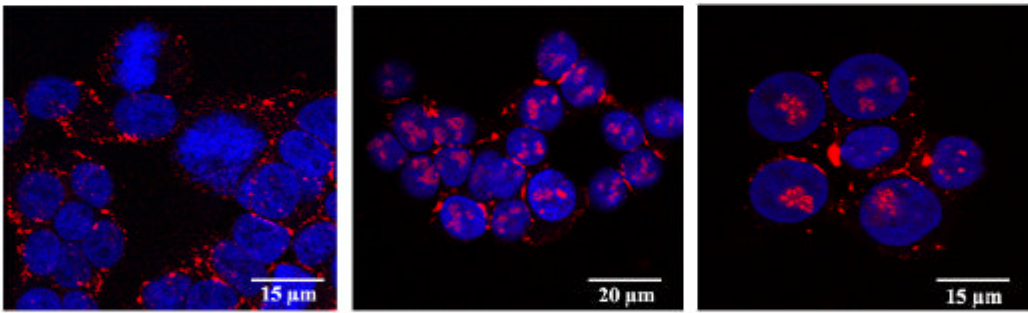
A



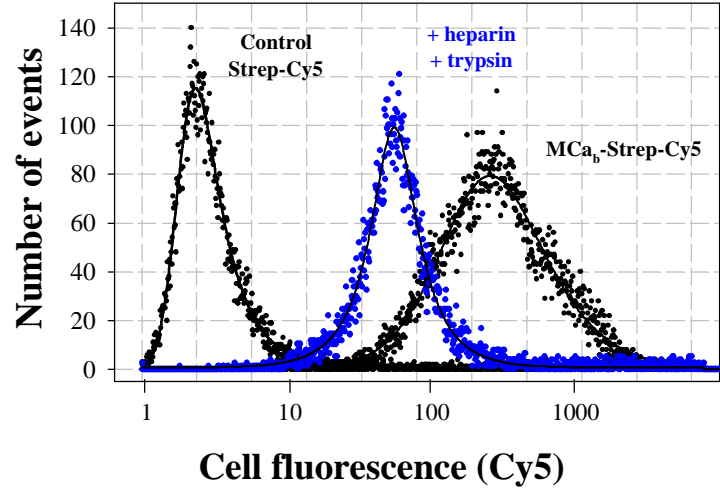
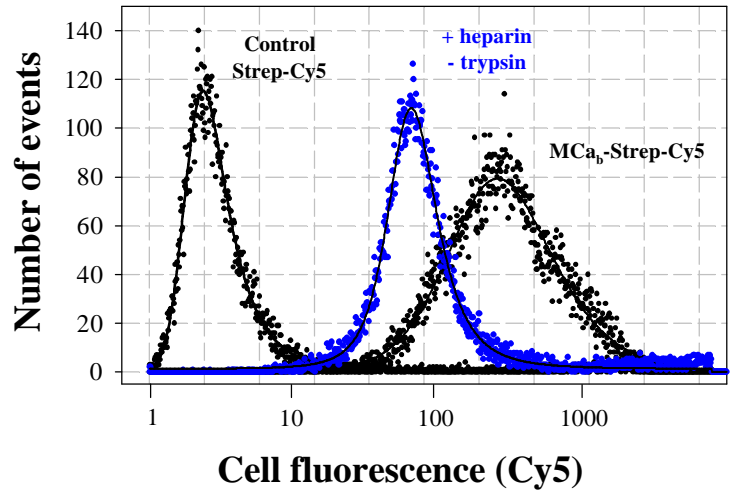
B



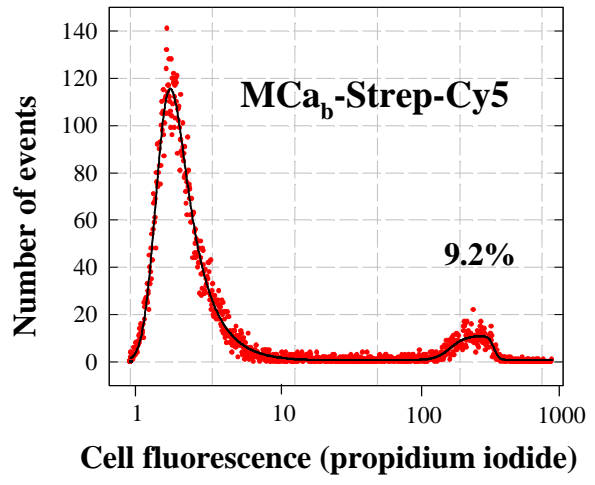
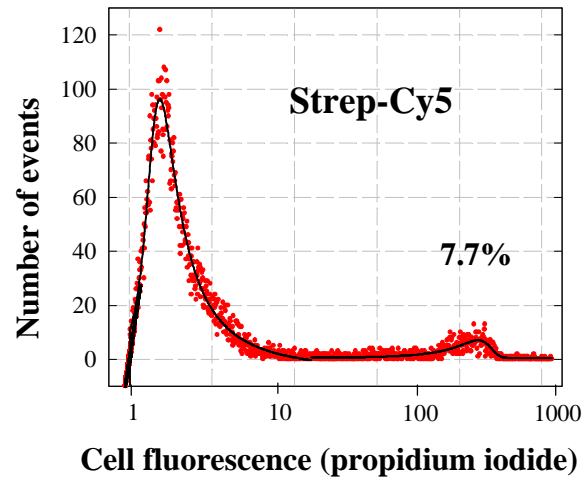
C



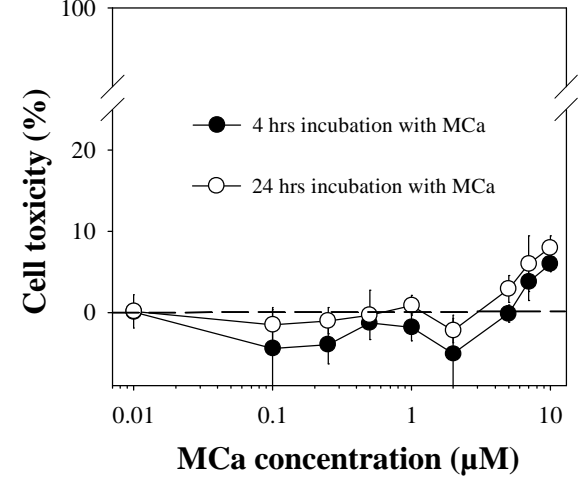
A



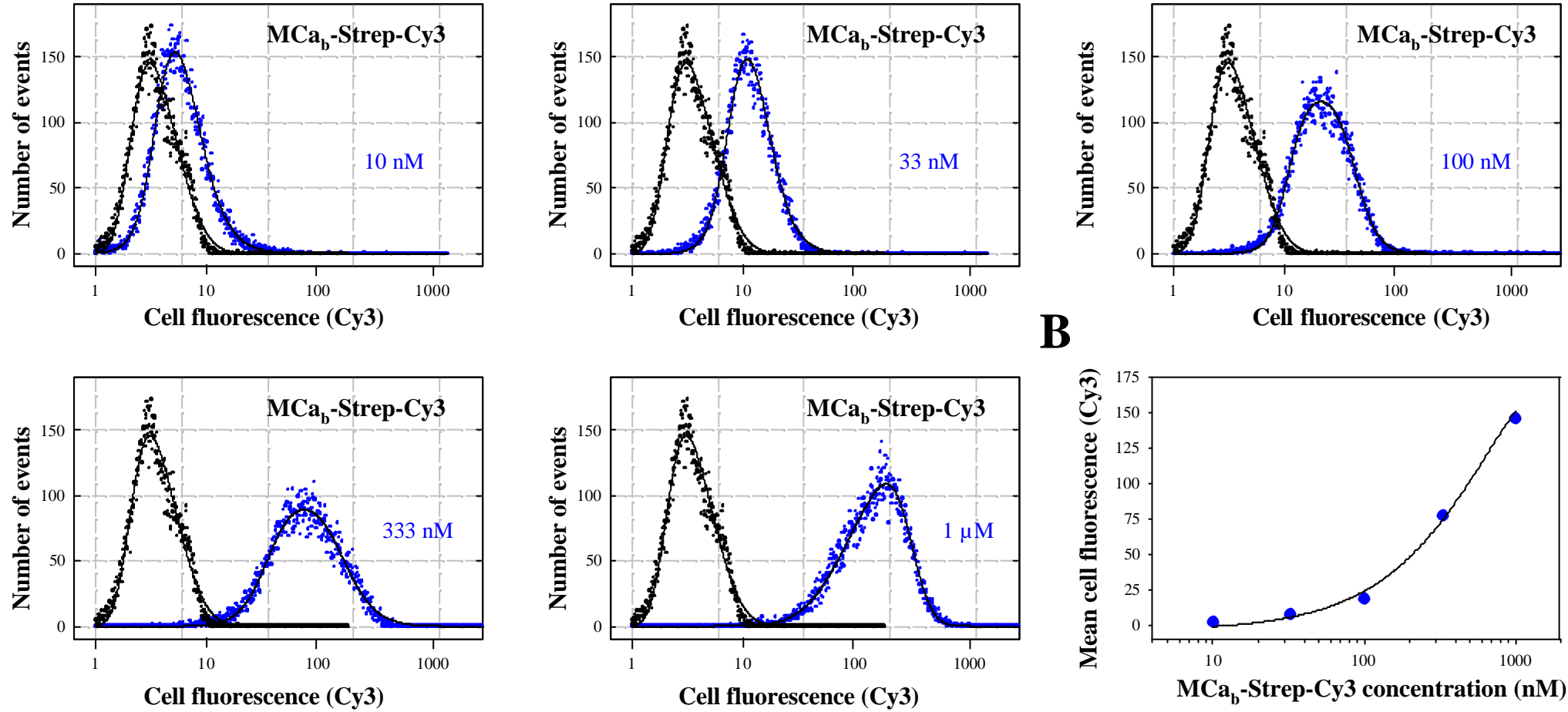
B



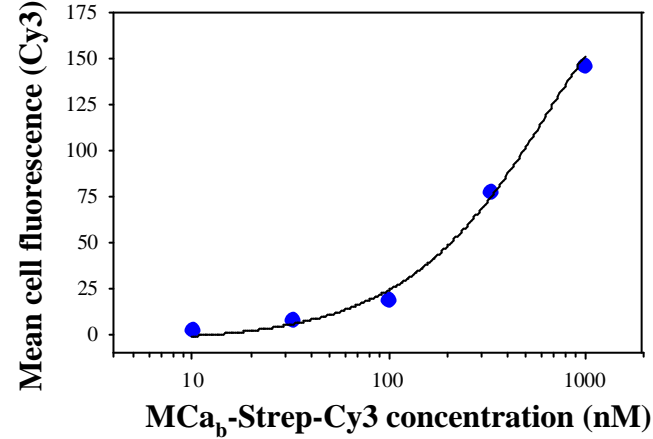
C



A

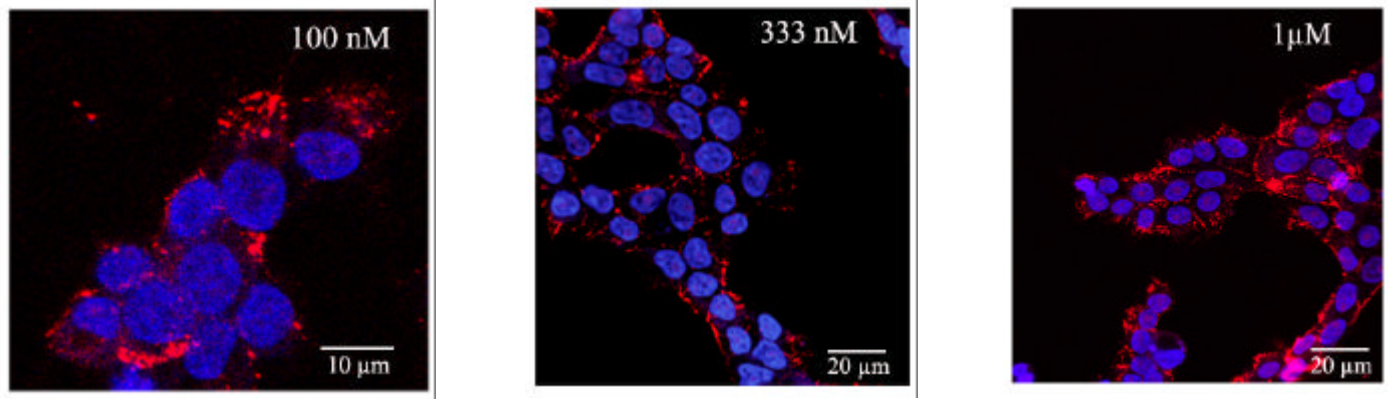


B

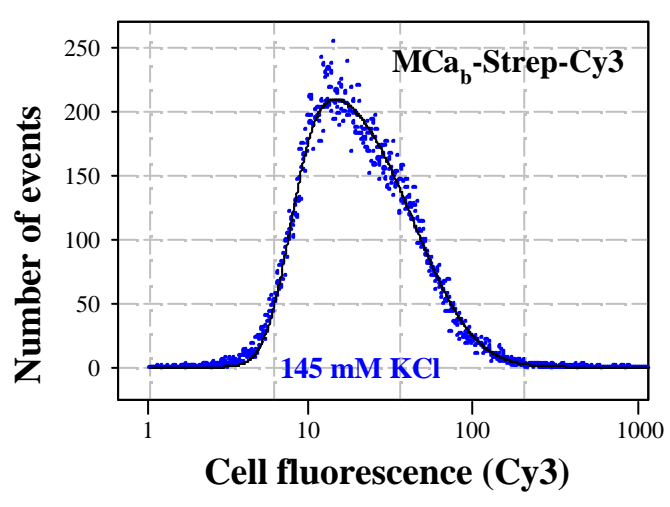
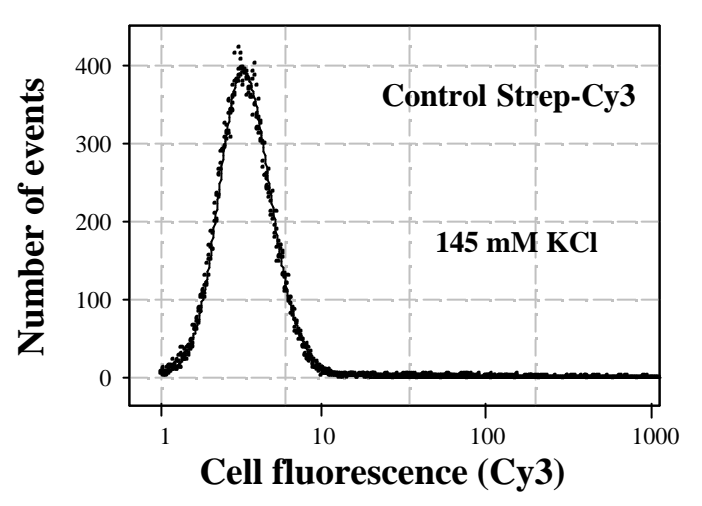
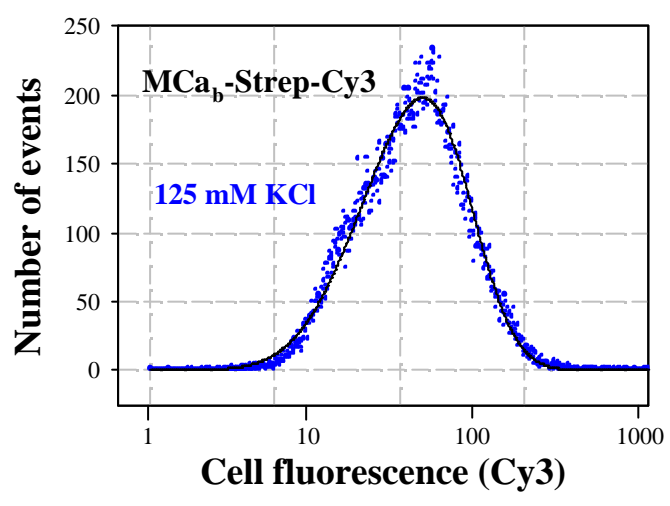
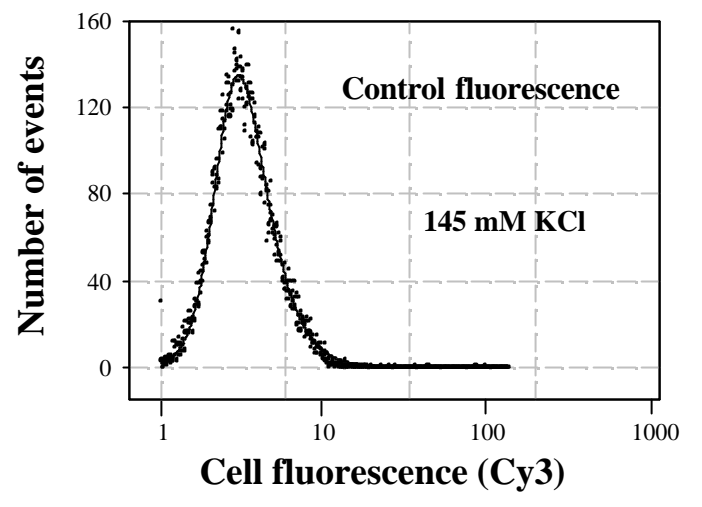
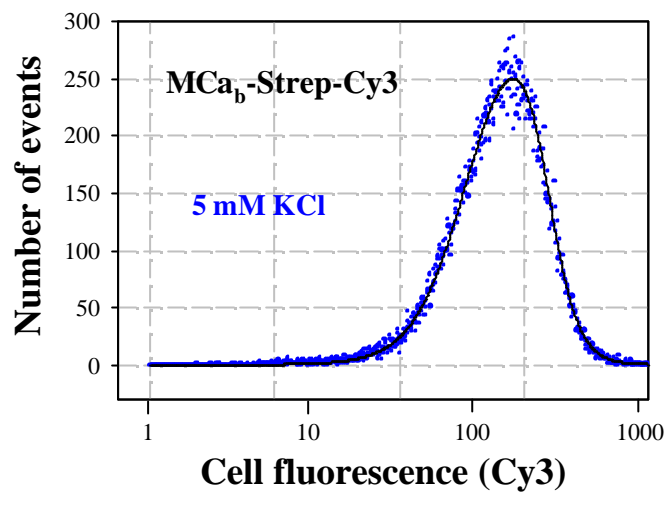


C

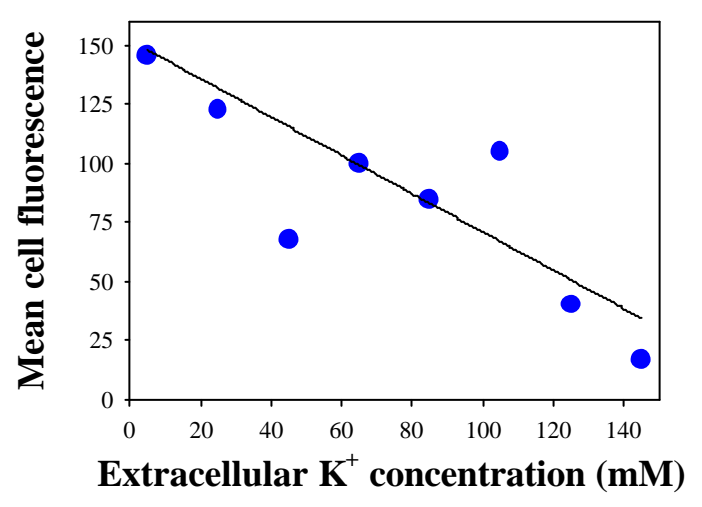
**MCA_b-Strep-Cy3
cell penetration**



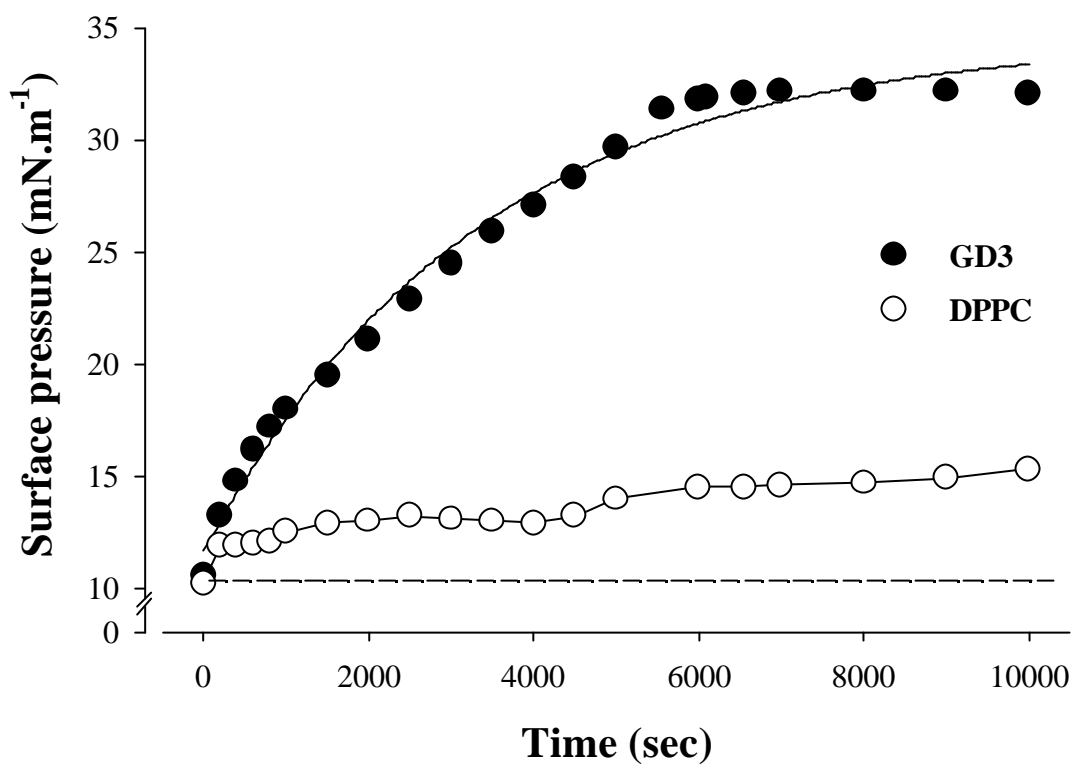
A



B



A



B

